

# Autonomous UAV Flight Navigation in Confined Spaces: A Reinforcement Learning Approach

Marco S. Tayar<sup>1</sup>, Lucas K. de Oliveira<sup>1</sup>, Juliano D. Negri<sup>1</sup>,  
Thiago H. Segreto<sup>1</sup>, Ricardo V. Godoy<sup>1</sup>, and Marcelo Becker<sup>1</sup>

**Abstract**— Inspecting confined industrial infrastructure, such as ventilation shafts, is a hazardous and inefficient task for humans. Unmanned Aerial Vehicles (UAVs) offer a promising alternative, but GPS-denied environments require robust control policies to prevent collisions. Deep Reinforcement Learning (DRL) has emerged as a powerful framework for developing such policies, and this paper provides a comparative study of two leading DRL algorithms for this task: the on-policy Proximal Policy Optimization (PPO) and the off-policy Soft Actor-Critic (SAC). The training was conducted with procedurally generated duct environments in Genesis simulation environment. A reward function was designed to guide a drone through a series of waypoints while applying a significant penalty for collisions. PPO learned a stable policy that completed all evaluation episodes without collision, producing smooth trajectories. By contrast, SAC consistently converged to a suboptimal behavior that traversed only the initial segments before failure. These results suggest that, in hazard-dense navigation, the training stability of on-policy methods can outweigh the nominal sample efficiency of off-policy algorithms. More broadly, the study provides evidence that procedurally generated, high-fidelity simulations are effective testbeds for developing and benchmarking robust navigation policies.

## I. INTRODUCTION

Manual inspection of industrial infrastructure, such as pipelines and ventilation ducts, is a hazardous, costly, and time-consuming process essential for operational integrity. Unmanned Aerial Vehicles (UAVs) present a transformative alternative, enabling rapid and safe data collection in environments inaccessible to humans. However, navigating a drone in an industrial duct presents unique challenges. In these environments, the close proximity of walls creates complex aerodynamic effects that increase collision risk [1], [2]. Figure 1 shows a real-world example of a test environment built to study these challenges. Classical motion planning methods often lack the adaptability needed for these unpredictable spaces, struggling to handle unmodeled aerodynamic phenomena such as the ground effect inside narrow pipes [3], [4]. This requires control policies that can learn and adapt to these complex dynamics.

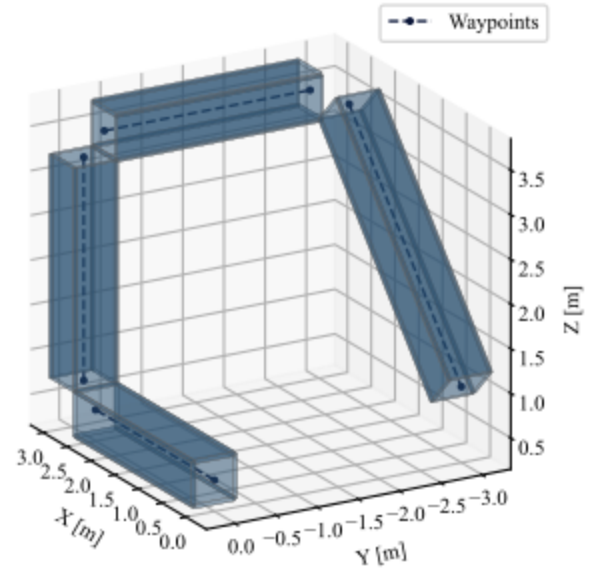
Deep Reinforcement Learning (DRL) offers a powerful alternative to these complex navigation problems. DRL agents

This work was supported by the Petróleo Brasileiro S/A - Petrobras, using resources from the R&D clause of the ANP, in partnership with the Universidade de São Paulo (USP) and the Fundação de Apoio à Física e à Química (FAFQ), under Cooperation Agreement No. 2023/00016-6 and 2023/00013-7.

<sup>1</sup>Marco S. Tayar, Lucas K. de Oliveira, Juliano D. Negri, Thiago H. Segreto, Ricardo V. Godoy, and Marcelo Becker are with the Department of Mechanical Engineering, University of São Paulo, São Carlos, Brazil. [becker@sc.usp.br](mailto:becker@sc.usp.br)



(a)



(b)

Fig. 1. Experimental setup for drone navigation in confined spaces (a), and its corresponding spatial representation (b).

can learn robust, end-to-end navigation policies directly from sensor data through trial-and-error. This approach has proven successful in autonomous drone applications and is well-suited for duct navigation [5], [6] due to its ability to generate adaptive behaviours without explicitly modeling complex

dynamics [7], [8], such as the aerodynamic interactions mentioned previously.

To address the challenge of performing autonomous UAV navigation in confined spaces, this paper investigates the application of DRL for learning stable flight control.

Our experiments were conducted in Genesis, an open-source simulator featuring a high-fidelity physics engine suitable for modeling the complex aerodynamic interactions central to this work. Within this simulated environment, we employed and contrasted two leading DRL algorithms from different learning paradigms: Proximal Policy Optimization (PPO) and Soft Actor-Critic (SAC). PPO, an on-policy algorithm, is chosen for its proven stability and robust performance in continuous control tasks [7]. In contrast, SAC, an off-policy algorithm, is selected for its high sample efficiency and effective exploration capabilities [8]. By comparing these distinct approaches, our goal is not merely to identify the most appropriate method in terms of performance, but to provide a comprehensive analysis of how on-policy and off-policy strategies contend with the challenges of confined-space navigation, thereby offering a broader evaluation of DRL's feasibility for this critical application. By training and evaluating both PPO and SAC agents in a high-fidelity simulation using the Genesis physics engine, this study aims to depict the potential of Genesis simulator in addressing complex environments and navigation tasks, such as UAV pipeline inspection and to compare the learning behaviours and final performance of on-policy versus off-policy algorithms in this constrained environment, while providing key insights into the challenges and potential of DRL as a practical solution for industrial inspection tasks.

## II. RELATED WORK

The use of UAVs for inspecting confined industrial spaces is a well-established alternative to dangerous manual methods [1], [9]. The academic literature confirms that navigating drones through these narrow settings presents significant technical hurdles. Research on autonomous flight in narrow tunnels and air ducts reveals that the close proximity of walls creates complex, unsteady aerodynamic disturbances that increase collision risk and challenge stable control [10], [3], [1], [11]. These works show that classical motion planning methods often fail because they cannot adapt to unmodeled phenomena, such as ground effect in the duct, suggesting the use of more advanced, adaptive control policies.

To address these challenges, numerous studies have demonstrated that Deep Learning (DL) architectures provide mechanisms capable of handling not only general narrow navigation tasks [12], [13], [14] but also more specialized problems [15], [16], such as the duct-following scenario. In this context, Deep Reinforcement Learning (DRL) has emerged as a leading paradigm for designing robust and adaptive control policies. DRL allows an agent to learn effective, end-to-end flight strategies directly from sensor data [5], [6], [17] through a process of trial-and-error, bypassing the need for explicit modeling of complex dynamics. The advantage of this approach has been demonstrated in

achieving superhuman performance in highly dynamic tasks like autonomous drone racing, proving its capability to solve complex control problems under extreme conditions [5], [17]. Further studies have also applied DRL to navigate cluttered and dynamic environments, reinforcing its suitability for unpredictable scenarios [6].

Within the DRL landscape, different algorithms offer distinct advantages. PPO is a state-of-the-art on-policy algorithm widely recognized for its stability and reliable performance across various tasks [7]. In contrast, SAC is a highly sample-efficient off-policy algorithm based on a maximum entropy framework, which makes it particularly effective for continuous control tasks like robotics [8]. While both PPO and SAC are prominent methods in autonomous navigation research [18], [6], a rigorous, direct comparison of their performance for the specific application of ensuring stable, collision-free flight in confined industrial ducts has remained an open research question. This study directly addresses this gap by empirically evaluating the trade-offs between PPO's stability and SAC's sample efficiency to identify the superior control policy for this industrial task.

## III. METHODS

### A. Simulation Environment

All experiments were conducted in the Genesis [19] physics engine, a platform enabling parallel, GPU-accelerated rigid-body simulation. The training environment features a duct, procedurally generated for each episode, to ensure the policy learns to navigate diverse and challenging scenarios.

Each duct is constructed as a sequence of  $N_s$  straight tubular segments connected end-to-end, as depicted in Figure 2. While the segments share a fixed radius of  $R_d = 0.25$  m and have stochastically determined lengths, their orientation is the key to creating complex paths. The angular deviation between consecutive tubes is randomized using Rodrigues' rotation formula [20], given by Equation 1. Specifically, the direction vector of a new segment is computed by applying a controlled rotation to the vector of the previous segment. This method ensures a continuous and natural change in the duct's path, emulating the structure of real-world pipelines.

$$\mathbf{v}' = \mathbf{v} \cos \theta + (\mathbf{k} \times \mathbf{v}) \sin \theta + \mathbf{k}(\mathbf{k} \cdot \mathbf{v})(1 - \cos \theta) \quad (1)$$

$\mathbf{v}$  is the vector to rotate,  $\mathbf{k}$  is the unit vector along the axis of rotation (the plane normal), and  $\theta$  is the rotation angle. Then, the generator outputs the walls and waypoints for each segment, which are then utilized in the simulation for both navigation and collision testing.

The waypoints  $\{\mathbf{w}_i\}_{i=1}^{N_w}$  are placed along the duct's centerline to guide the agent through these generated courses. The agent controls a simulated Bitcraze Crazyflie 2 (CF2), a  $92 \times 92 \times 29$  mm nano-quadcopter (Figure 3), though the framework supports any UAV via URDF import.

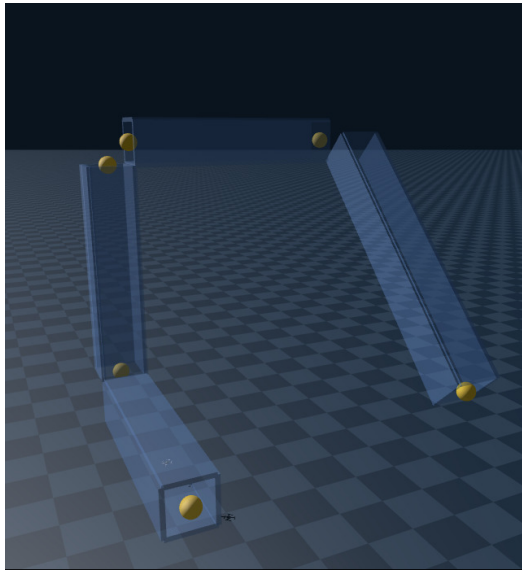


Fig. 2. A procedurally generated duct environment in Genesis, composed of connected tubular segments with varying orientations.

### B. State and Action Representation

The state vector  $s_t \in \mathbb{R}^{20}$  at time  $t$  aggregates geometric, kinematic, and actuation history information is obtained using Equation 2.

$$s_t = [\mathbf{p}_{rel}, \hat{\mathbf{p}}_{rel}^B, \mathbf{q}, \mathbf{v}_{lin}^B, \mathbf{v}_{ang}^B, \mathbf{a}_{t-1}], \quad (2)$$

where  $\mathbf{p}_{rel} \in \mathbb{R}^3$  is the position vector from the UAV to the next waypoint,  $\hat{\mathbf{p}}_{rel}^B$  is its unit-normalized form expressed in the body frame B,  $\mathbf{q} \in \mathbb{R}^4$  is the unit quaternion describing

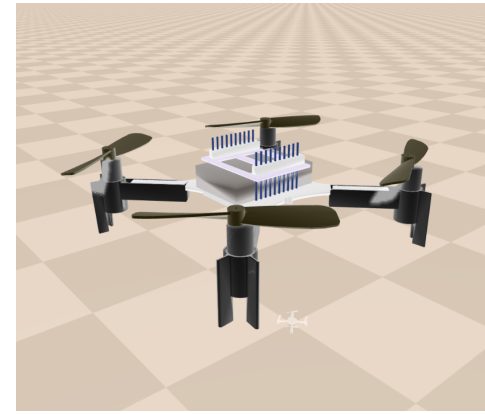


Fig. 3. The simulated Crazyflie 2 (CF2) UAV used for all experiments.

world-to-body orientation,  $\mathbf{v}_{lin}^B, \mathbf{v}_{ang}^B \in \mathbb{R}^3$  are body-frame linear and angular velocities, and  $\mathbf{a}_{t-1} \in \mathbb{R}^4$  is the previous motor command vector. The continuous action vector  $a_t \in [-1, 1]^4$  is mapped to individual rotor speeds via Equation 3.

$$\omega_i = (1 + 0.8 a_{t,i}) \omega_{hover} \quad (3)$$

for  $i = 1, \dots, 4$ , where  $\omega_{hover}$  is the minimum angular velocity required for the drone to counteract gravity and maintain a stable hover. For this specific drone model, the hover speed is calibrated to a value of 14468.43 RPM.

### C. Reward Formulation

The reward function is a critical component for guiding the agent's learning process. To address the multi-faceted nature of the UAV navigation task, a composite reward function,  $R_t$ ,

TABLE I  
DEFINITION OF REWARD TERMS FOR THE UAV NAVIGATION TASK, BASED ON SECTION III-C.

	Reward Term	Function	Weights		Notes
			PPO	SAC	
Guidance	Progress	$(\mathbf{v}_{lin}^B \cdot \Delta t) \cdot \frac{\ \mathbf{p}_{rel}\ }{\ \mathbf{p}_{rel}\ }$	25.0	50.0	Rewards movement toward the next waypoint.
	Centerline Deviation	$-\frac{\ p_t - c_t\ }{R_d}$	5.0	10.0	Penalizes distance from the duct centerline.
	Velocity Tracking	$\exp(-\beta_v \ \mathbf{v}_{lin}^B - v^*\ )$	3.0	4.0	Encourages maintaining a target forward velocity $v^*$ .
Stability	Orientation Alignment	$\frac{\alpha_y f_B^\top d_h + \alpha_\ell u_B^\top u_W}{\alpha_y + \alpha_\ell}$	10.0	10.0	Rewards correct yaw and level attitude.
	Angular Vel. Damping	$-\ \mathbf{v}_{ang}^B\ ^2$	8.5e-3	8.5e-3	Penalizes high rotational speeds.
	Action Smoothness	$-\ \mathbf{a}_t - \mathbf{a}_{t-1}\ ^2$	7.0e-3	7.0e-3	Penalizes abrupt changes in motor commands.
Event-based	Waypoint Pass	$\mathbb{I}[\ \mathbf{p}_{rel}\  < 1.5 R_d]$	22.0	22.0	A sparse bonus for reaching a waypoint's proximity.
	Duct Finish	$\mathbb{I}[\text{all waypoints passed}]$	50.0	50.0	A large terminal bonus for completing the course.
	Crash Penalty	$-\mathbb{I}[\text{termination}]$	17.0	17.0	A large terminal penalty for any collision or violation.

was designed and computed at each timestep as a weighted sum of several terms:

$$R_t = \sum_k w_k r_k, \quad (4)$$

where  $r_k$  represents an individual reward component and  $w_k \in \mathbb{R}^+$  is its corresponding weight, detailed in [Table I](#). This modular structure is common in robotics, as it allows for the decomposition of a complex task into more manageable sub-objectives [\[21\], \[22\]](#). The formulation is divided into three distinct categories. **Guidance rewards** provide a dense signal to direct the agent along the desired path by rewarding forward *Progress*, penalizing *Centerline Deviation*, and encouraging *Velocity Tracking* [\[23\]](#). Complementing this, **Stability rewards** act as a regularization to promote physically plausible and safe flight, constraining *how* the task is performed. These include terms for maintaining proper *Orientation Alignment*, damping high *Angular Velocity*, and ensuring *Action Smoothness* to prevent abrupt motor commands, which is a standard practice for robust control in locomotion tasks [\[22\], \[21\]](#). Finally, **Event-based rewards** deliver sparse, high-magnitude signals for critical discrete events, such as a bonus for a *Waypoint Pass*, a large terminal reward for *Duct Finish*, or a significant penalty for a *Crash* [\[21\]](#).

The weights  $w_k$  were empirically determined, with a notable adjustment between the PPO and SAC agents. It is known that off-policy algorithms such as SAC, which learn from a diverse replay buffer, can exhibit different sensitivities to reward scaling compared to on-policy methods [\[24\]](#). A hypothesis was formed that a stronger signal for the primary task objectives could improve learning from the varied experiences in the buffer. Consequently, the weights for the main guidance terms (*Progress* and *Centerline Deviation*) were increased for SAC. Despite this principled adjustment, the agent performance remained suboptimal, as discussed in [section IV](#).

#### D. Learning Algorithms

Two learning paradigms were compared. For the on-policy case, PPO was implemented via `rsl-r1` with an actor-critic network of two hidden layers (256, 128 units, ELU activations), rollout horizon 256, 4096 parallel environments, adaptive KL target 0.01,  $\gamma = 0.99$ ,  $\lambda = 0.95$ , and clipping parameter  $\epsilon = 0.2$ . For the off-policy case, SAC was implemented in `Stable-Baselines3` with an actor and twin critics sharing the same architecture, replay buffer size  $10^6$ , batch size 512, target update coefficient  $\tau = 0.005$ , discount  $\gamma = 0.99$ , automatic entropy tuning, and a learning rate linearly decayed from  $3 \times 10^{-2}$  to zero over  $10^6$  timesteps. These hyperparameters were selected based on the standard configurations provided by their respective libraries, which are established as robust baselines for continuous control tasks.

## IV. RESULTS

### A. PPO Training

The training progression of the PPO agent, detailed in [Table II](#), demonstrates a convergence to a robust and effective navigation policy. Early in the training, by the first checkpoint (100 iterations), the agent had already achieved a 100% course completion rate with zero collisions. This indicates that the fundamental task of traversing the duct without catastrophic failure was learned quickly, validating the efficacy of the reward function's core guidance and penalty terms.

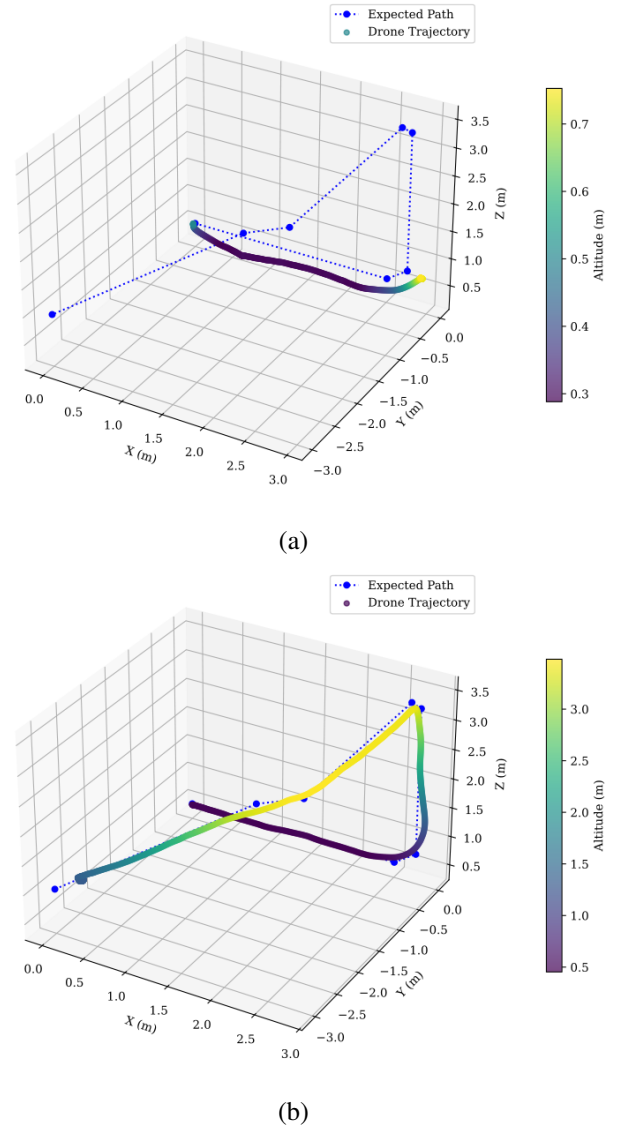


Fig. 4. Comparison of drone trajectories at different stages of PPO training. Subfigure (a) shows a less stable path from an early checkpoint, while subfigure (b) shows a much smoother and more precise path from a mature model.

The subsequent training phase focused on refining the agent's control policy for improved precision and stability ([Figure 4](#)). A significant enhancement in flight quality is observed between checkpoints 200 and 300, where the Average

Deviation from the centerline was nearly halved, decreasing from 0.1128 m to 0.0636 m. This period corresponds to the agent learning to minimize lateral drift and maintain a more centered trajectory, a critical behavior for navigating narrow passages. The policy continued to optimize, reaching its peak performance at checkpoint 400, where it recorded the highest Average Reward (10.2k) and maintained a low average deviation. The slight performance degradation at the final checkpoint (500) may suggest minor overfitting or the policy settling into a slightly different but equally successful equilibrium. Overall, the PPO agent demonstrated a classic learning pattern: mastering the primary objective first, followed by a clear phase of trajectory optimization, resulting in a highly stable and precise final policy.

### B. SAC Training

In contrast to PPO, the Soft Actor-Critic (SAC) agent failed to develop a successful end-to-end navigation policy, as evidenced by the performance metrics in [Table III](#). Throughout the entire training process of 650k timesteps, the Course Finish Rate remained at 0.0%, with the agent consistently failing to traverse the entire duct system. Collisions were persistent, with an average of 1.00 per episode, indicating that terminal failure was the standard outcome.

Despite this overarching failure, the data reveals that the agent did engage in a learning process. The Average Reward shows a consistent upward trend, increasing from 2.0k to 5.4k. This improvement is correlated with the agent's ability to navigate a limited portion of the course, successfully passing a maximum of two waypoints before crashing. This behavior is characteristic of an off-policy agent converging to a local optimum. The replay buffer, heavily populated with experiences from the initial, simpler segments of the duct, likely biased the agent towards perfecting the start of the trajectory at the expense of discovering strategies to overcome later challenges. The sample efficiency of SAC,

therefore, proved counterproductive in this context, as it led the agent to over-specialize on a suboptimal, incomplete behavior pattern without the broader ([Figure 5](#)), on-policy exploration needed to find a globally successful solution.

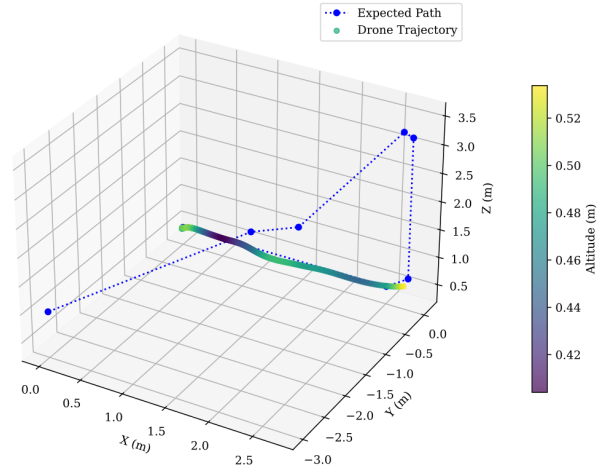


Fig. 5. The drone trajectory that achieves the best performance for a model trained with SAC algorithm after 530,000 training steps.

## V. CONCLUSION

This paper successfully demonstrated the feasibility of using Deep Reinforcement Learning to generate robust control policies for autonomous drone navigation within narrow, confined industrial ducts. By leveraging a high-fidelity physics simulator, it was established that a DRL agent can implicitly learn to manage the complex aerodynamic interactions present in confined spaces. The resulting on-policy agent achieved consistent, collision-free trajectories, validating that DRL can produce the stable and precise policies required for real-world industrial inspection.

TABLE II  
MODEL PERFORMANCE METRICS BY TRAINING CHECKPOINT

Metric	Checkpoint 100	Checkpoint 200	Checkpoint 300	Checkpoint 400	Checkpoint 500
Average Reward	9.4k	8.1k	9.9k	10.2k	8.6k
Avg. Waypoints Passed	7.00 / 7	7.00 / 7	7.00 / 7	7.00 / 7	7.00 / 7
Avg. Collisions/Episode	0.00	0.00	0.00	0.00	0.00
Average Deviation (m)	0.1226	0.1128	0.0636	0.0646	0.094
Maximum Deviation (m)	0.2318	0.2191	0.1505	0.1822	0.2390

TABLE III  
SAC PERFORMANCE METRICS FOR SELECTED TRAINING CHECKPOINTS

Metric	Checkpoint 130k	Checkpoint 260k	Checkpoint 390k	Checkpoint 520k	Checkpoint 650k
Average Reward	2.0k	3.0k	3.6k	4.1k	5.4k
Avg. Waypoints Passed	0 / 7	1 / 7	2 / 7	2 / 7	2 / 7
Avg. Collisions/Episode	1.00	1.00	1.00	0.00	1.00
Average Deviation (m)	0.0370	0.0490	0.0651	0.1560	0.0577
Maximum Deviation (m)	0.0752	0.1169	0.1919	0.1995	0.1122

The implementation process provided critical insights into the practical challenges and potential of this approach. The primary challenge identified was ensuring sufficient exploration to discover a complete, end-to-end flight path in an environment where catastrophic failures (collisions) are common. The performance difference between the on-policy (PPO) and off-policy (SAC) agents served to highlight this issue, revealing that the learning strategy is as important as the learning algorithm itself. For high-stakes sequential tasks, these findings suggest that the stability afforded by on-policy data collection can be paramount for success. This work thus offers key insights into the practical application of DRL for industrial tasks, moving beyond theoretical performance to address implementation-specific hurdles.

This development in a realistic simulation serves as a first step toward real-world deployment and validates DRL as a powerful paradigm for automating complex navigation tasks. The primary focus of future work will be bridging the simulation-to-reality (sim-to-real) gap to transfer the successful PPO policy to the physical testbed. To achieve this, several enhancements are planned for the simulator, including the incorporation of domain randomization to create a policy robust to physical-world variations not perfectly captured in simulation, such as sensor noise and aerodynamic effects. Furthermore, curriculum learning strategies will be implemented to progressively increase task difficulty, thereby creating a more robust and generalizable agent. These improvements will serve to investigate hybrid approaches that improve the exploratory capabilities of off-policy agents in similarly constrained environments.

## REFERENCES

- [1] T. Martin, A. Guénard, V. Tempez, L. Renaud, T. Raharijaona, F. Ruffier, and J.-B. Mouret, “Flying in air ducts,” *npj Robotics*, vol. 3, no. 1, p. 16, 2025.
- [2] C. Powers, D. Mellinger, A. Kushleyev, B. Kothmann, and V. Kumar, “Influence of aerodynamics and proximity effects in quadrotor flight,” in *Experimental Robotics: The 13th International Symposium on Experimental Robotics*. Springer, 2013, pp. 289–302.
- [3] L. Wang, Y. Ning, H. Chen, P. Liu, Y. Xu, H. Xu, X. Lyu, and S. Shen, “Autonomous flights inside narrow tunnels,” *IEEE Transactions on Robotics*, 2025.
- [4] A. Betz, “The ground effect on lifting propellers,” NASA Technical Reports Server, Tech. Rep., 1937.
- [5] E. Kaufmann, L. Bauersfeld, A. Loquercio, M. Müller, V. Koltun, and D. Scaramuzza, “Champion-level drone racing using deep reinforcement learning,” *Nature*, vol. 620, no. 7976, pp. 982–987, 2023.
- [6] Y. Sheng, H. Liu, J. Li, and Q. Han, “Uav autonomous navigation based on deep reinforcement learning in highly dynamic and high-density environments,” *Drones*, vol. 8, no. 9, 2024. [Online]. Available: <https://www.mdpi.com/2504-446X/8/9/516>
- [7] J. Schulman, F. Wolski, P. Dhariwal, A. Radford, and O. Klimov, “Proximal policy optimization algorithms,” *arXiv preprint arXiv:1707.06347*, 2017.
- [8] T. Haarnoja, A. Zhou, P. Abbeel, and S. Levine, “Soft actor-critic: Off-policy maximum entropy deep reinforcement learning with a stochastic actor,” in *Proceedings of the 35th International Conference on Machine Learning*, ser. Proceedings of Machine Learning Research, J. Dy and A. Krause, Eds., vol. 80. PMLR, 10–15 Jul 2018, pp. 1861–1870. [Online]. Available: <https://proceedings.mlr.press/v80/haarnoja18b.html>
- [9] T. Özaslan, G. Loianno, J. Keller, C. J. Taylor, V. Kumar, J. M. Wozencraft, and T. Hood, “Autonomous navigation and mapping for inspection of penstocks and tunnels with mavs,” *IEEE Robotics and Automation Letters*, vol. 2, no. 3, pp. 1740–1747, 2017.
- [10] L. Bauersfeld and D. Scaramuzza, “Low-latency event-based velocimetry for quadrotor control in a narrow pipe,” *arXiv preprint arXiv:2507.15444*, 2025.
- [11] S. A. Conyers, “Empirical evaluation of ground, ceiling, and wall effect for small-scale rotorcraft,” Ph.D. dissertation, University of Denver, 2019.
- [12] D. Gandhi, L. Pinto, and A. Gupta, “Learning to fly by crashing,” 2017. [Online]. Available: <https://arxiv.org/abs/1704.05588>
- [13] F. Affonso, F. Andrade, G. Capezzuto, M. V. Gasparino, G. Chowdhary, and M. Becker, “Crow: A self-supervised crop row navigation algorithm for agricultural fields,” *Journal of Intelligent & Robotic Systems*, vol. 111, no. 1, Feb 2025. [Online]. Available: <https://link.springer.com/article/10.1007/s10846-025-02219-2#citeas>
- [14] F. A. Pinto, F. A. G. Tommaselli, M. V. Gasparino, and M. Becker, “Navigating with finesse: Leveraging neural network-based lidar perception and ilqr control for intelligent agriculture robotics,” in *2023 Latin American Robotics Symposium (LARS), 2023 Brazilian Symposium on Robotics (SBR), and 2023 Workshop on Robotics in Education (WRE)*, 2023, pp. 502–507.
- [15] H. Karan, E. Yang, D. Farkash, G. Warnell, J. Biswas, and P. Stone, “Sterling: Self-supervised terrain representation learning from unconstrained robot experience,” 2023. [Online]. Available: <https://arxiv.org/abs/2309.15302>
- [16] A. Sivakumar, N. Wang, F. Andrade, G. Tommaselli, M. Gasparino, M. Becker, and G. Chowdhary, “Cropfollowrl: Learning under-canopy navigation policy with keypoints abstraction,” in *nature-bots.github.io*, 2024. [Online]. Available: [https://nature-bots.github.io/assets/camera-ready/CropFollowRL\\_Arun.pdf](https://nature-bots.github.io/assets/camera-ready/CropFollowRL_Arun.pdf)
- [17] Y. Song, A. Romero, M. Müller, V. Koltun, and D. Scaramuzza, “Reaching the limit in autonomous racing: Optimal control versus reinforcement learning,” *Science Robotics*, vol. 8, no. 82, p. eadg1462, 2023.
- [18] D. Hanover, A. Loquercio, L. Bauersfeld, A. Romero, R. Penicka, Y. Song, G. Cioffi, E. Kaufmann, and D. Scaramuzza, “Autonomous drone racing: A survey,” *IEEE Transactions on Robotics*, vol. 40, pp. 3044–3067, 2024.
- [19] G. Authors, “Genesis: A generative and universal physics engine for robotics and beyond,” December 2024. [Online]. Available: <https://github.com/Genesis-Embodied-AI/Genesis>
- [20] X. Kan, J. Thomas, H. Teng, H. G. Tanner, V. Kumar, and K. Karydis, “Analysis of ground effect for small-scale uavs in forward flight,” *IEEE Robotics and Automation Letters*, vol. 4, no. 4, pp. 3860–3867, 2019.
- [21] J. Hwangbo, J. Lee, A. Dosovitskiy, D. Bellicoso, V. Tsounis, V. Koltun, and M. Hutter, “Learning agile and dynamic motor skills for legged robots,” *Science Robotics*, vol. 4, no. 26, p. eaau5872, 2019.
- [22] J. Tan, T. Zhang, E. Coumans, A. Iscen, Y. Bai, D. Hafner, S. Bohez, and V. Vanhoucke, “Sim-to-real: Learning agile locomotion for quadruped robots,” in *Proceedings of Robotics: Science and Systems (RSS)*, Pittsburgh, Pennsylvania, June 2018.
- [23] E. Kaufmann, A. Loquercio, R. Ranftl, A. Dosovitskiy, V. Koltun, and D. Scaramuzza, “Deep drone racing: From simulation to reality with domain randomization,” *IEEE Transactions on Robotics*, vol. 36, no. 5, pp. 1375–1390, 2020.
- [24] T. Haarnoja, A. Zhou, P. Abbeel, and S. Levine, “Soft actor-critic: Off-policy maximum entropy deep reinforcement learning with a stochastic actor,” in *Proceedings of the 35th International Conference on Machine Learning (ICML)*, ser. Proceedings of Machine Learning Research, vol. 80. PMLR, 10–15 Jul 2018, pp. 1861–1870.